Figure S1. Cell viability of NCM460 cells following treatment with 0-50 μM CVB-D for 24 or 48 h. CVB-D, cyclovirobuxine D.

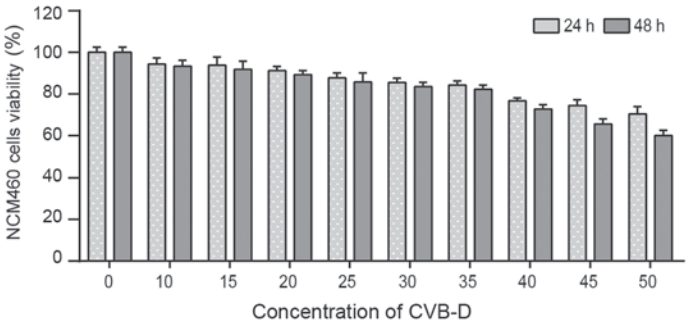

Figure S2. Expression levels of CD133 and cyclin D1 decreased with increasing concentrations of CVB-D (0-40 μM), as detected by western blotting. Data are presented as mean ± standard deviation (n=3). *P<0.05, **P<0.01 vs. control group (0 μM CVB-D). CVB-D, cyclovirobuxine D.

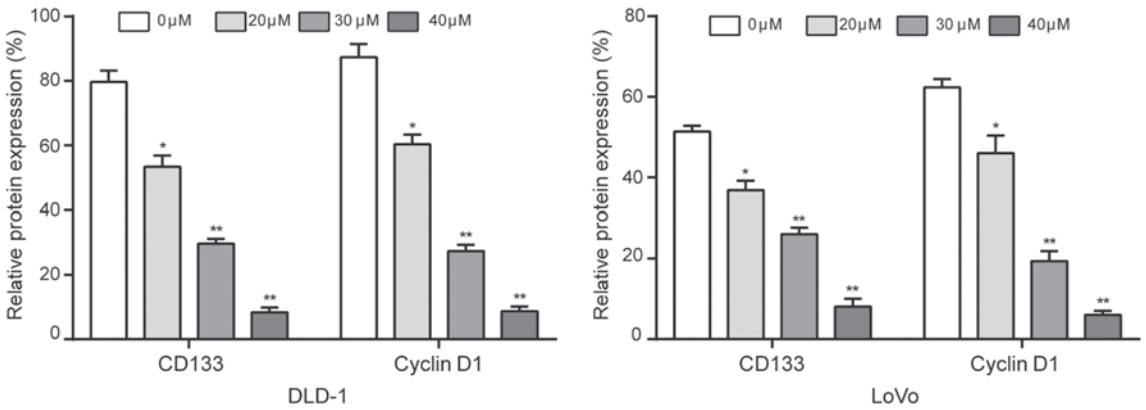

Figure S3. Expression levels of Bcl-2 and Bax following treatment with CVB-D (0-40 μM), as detected by western blotting. Data are presented as mean ± standard deviation (n=3). *P<0.05, **P<0.01 vs. control group (0 μM CVB-D). CVB-D, cyclovirobuxine D; Bcl-2, B-cell lymphoma 2; Bax, Bcl-2-associated X protein.

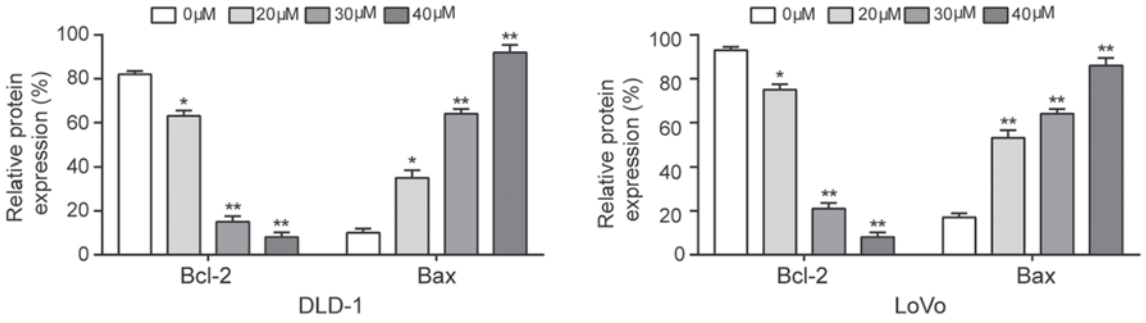

Figure S4. Analysis of transcription factors in GEPIA2. (A) The expression levels of transcription factors (Snail, Slug, ZEB1 and ZEB2) in COAD (red) and normal tissue (gray). (B) The significant association between transcription factors and OS rate in COAD. *P<0.05. COAD, colon adenocarcinoma; OS, overall survival.

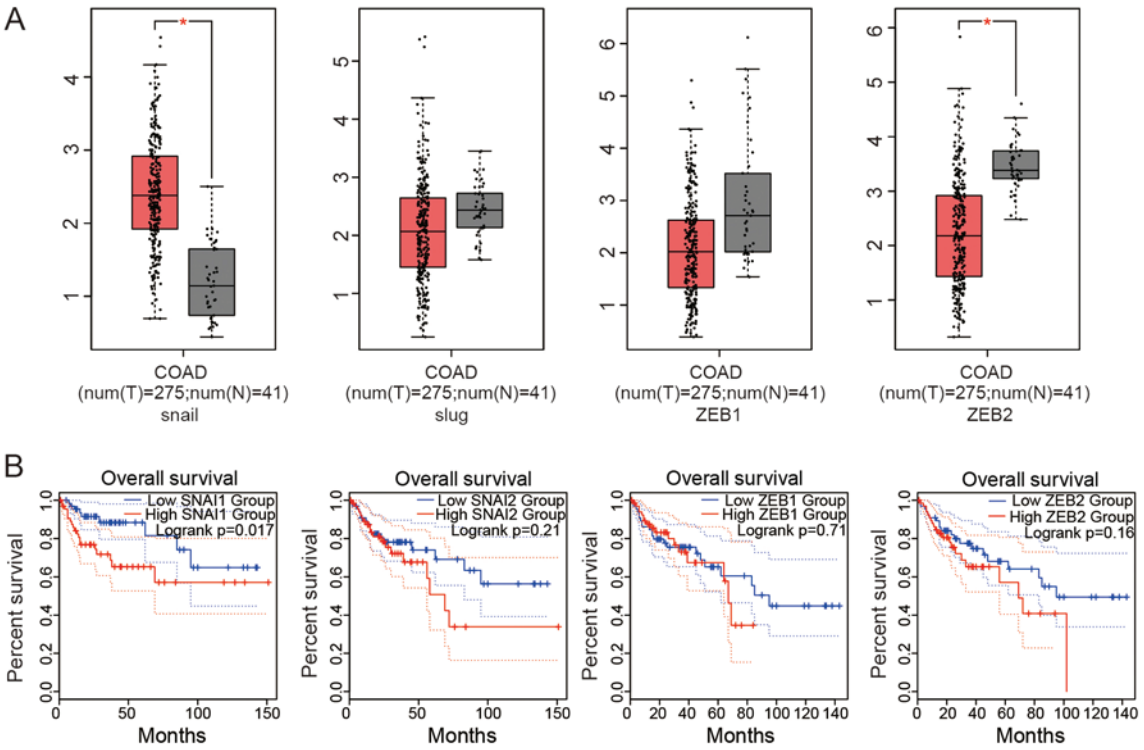

Figure S5. Expression levels of PI3K, p-AKT, AKT, p-ERK, ERK and Snail following after treatment of CRC cells with CVB-D (0-40 μM) for 48 h. β-actin was used as the loading control. Data are presented as mean ± standard deviation (n=3). *P<0.05, **P<0.01 vs. control group (0 μM CVB-D). CVB-D, cyclovirobuxine D; p-, phosphorylated; CRC, colorectal cancer.

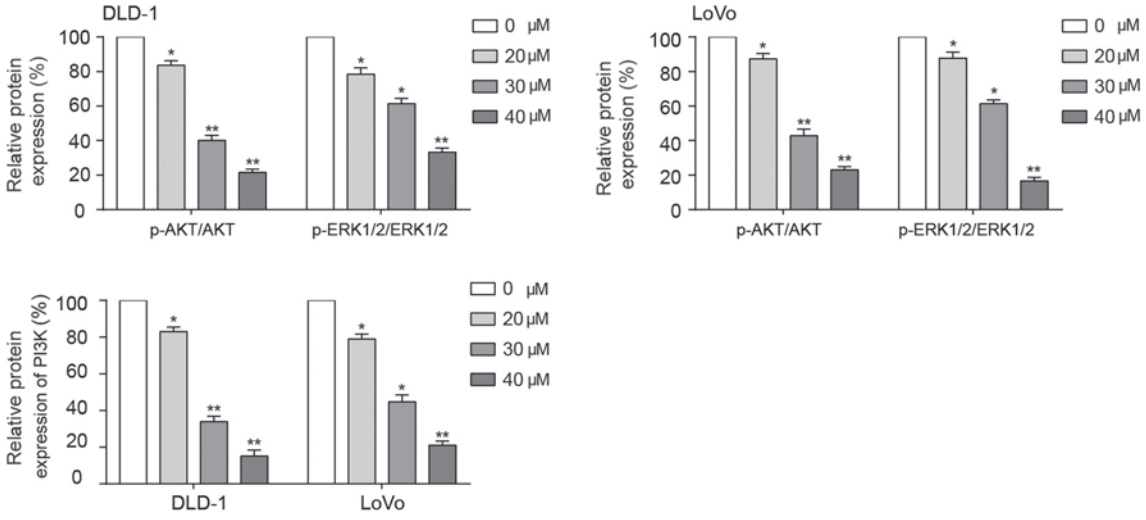

Figure S6. Expression of 24 differentially expressed genes in COAD (red) and adjacent normal tissues (grey). *P<0.05. COAD, colon adenocarcinoma.

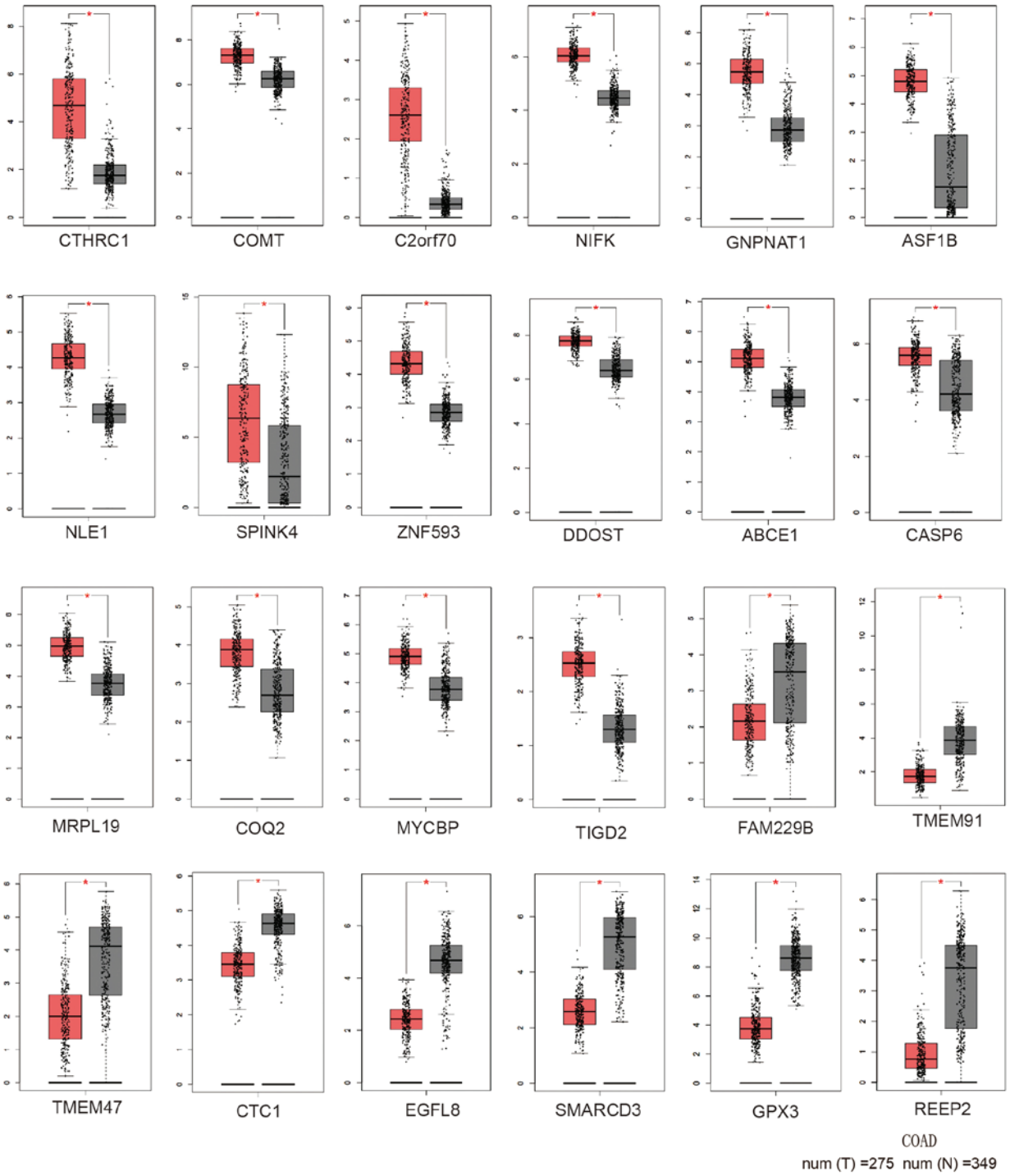

Figure S7. Associations between 24 differentially expressed genes and the overall survival of patients with colon adenocarcinoma.

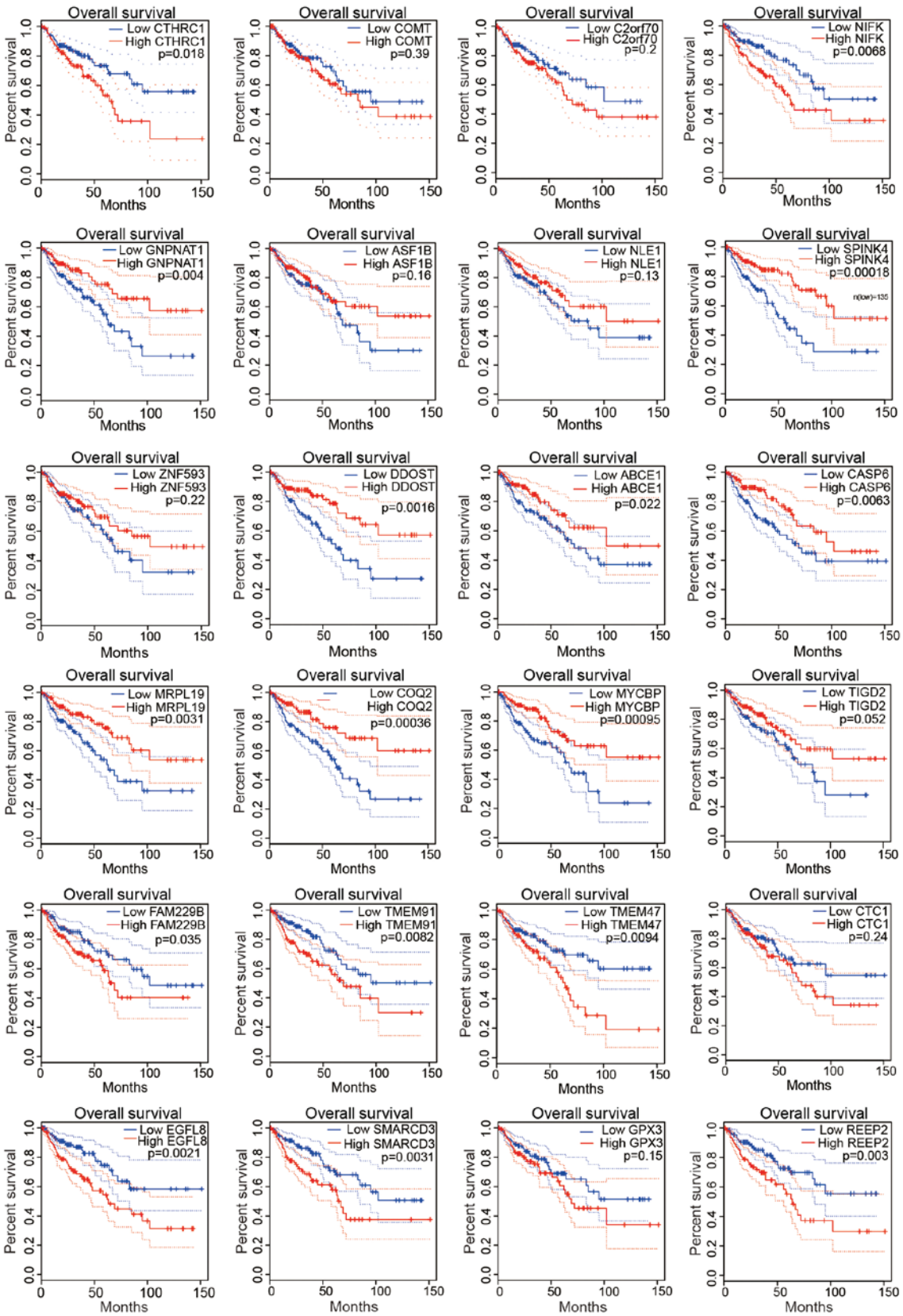

Figure S8. Associations between 24 differentially expressed genes and the disease-free survival of patients with colon adenocarcinoma.

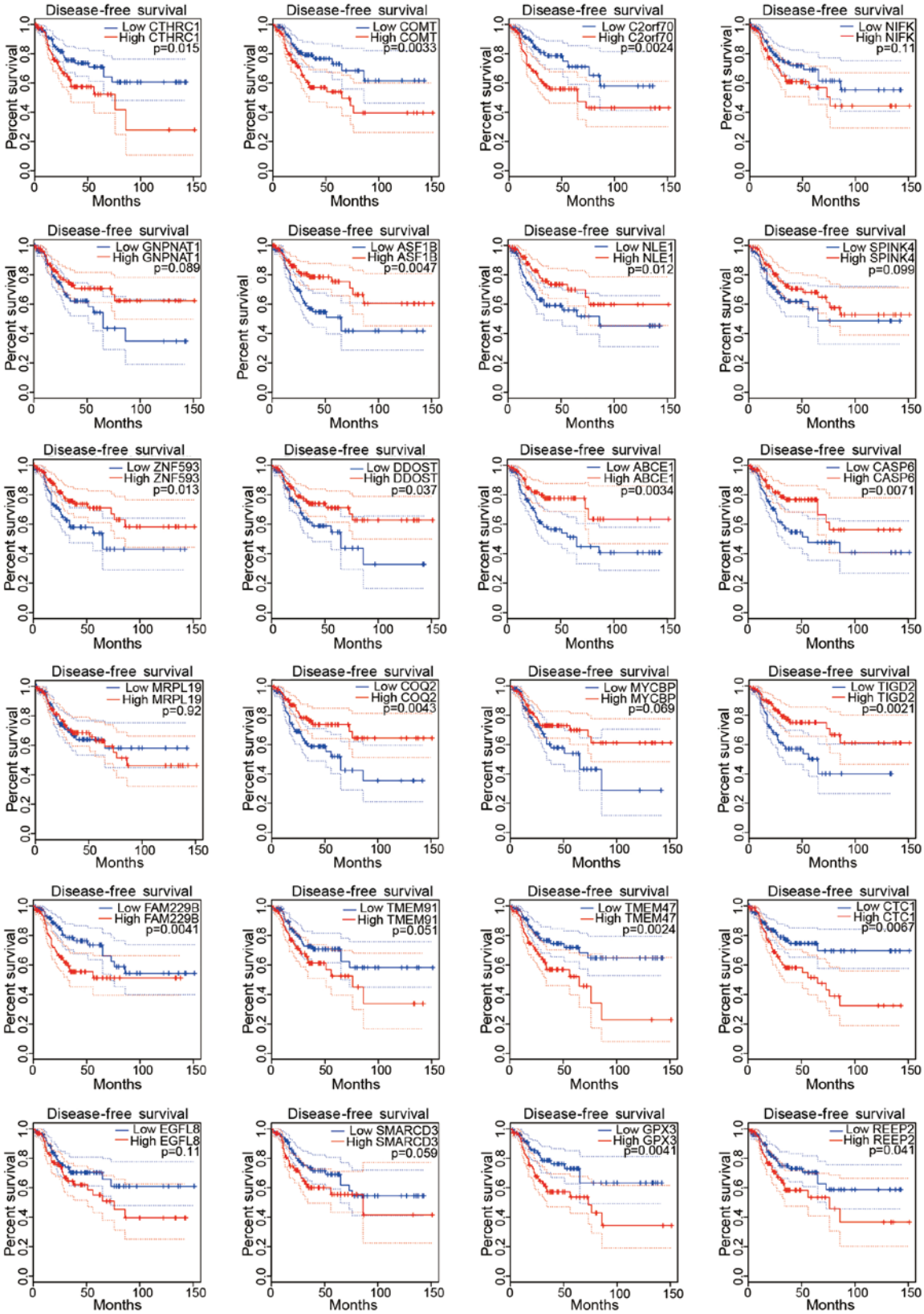

Figure S9. Analysis of the correlation between transcription factors and CTHRC1, COMT, C2orf70 and NIFK. (A) Analysis of the correlation between Snail and CTRC1, COMT, C2orf70 and NIFK. (B) Analysis of the correlation between Slug and CTRC1, COMT, C2orf70 and NIFK. (C) Analysis of the correlation between ZEB1 and CTRC1, COMT, C2orf70 and NIFK. (D) Analysis of the correlation between ZEB2 and CTRC1, COMT, C2orf70 and NIFK. CTHRC1, collagen triple helix repeat containing 1; ZEB, zinc finger E-box-binding homeobox.

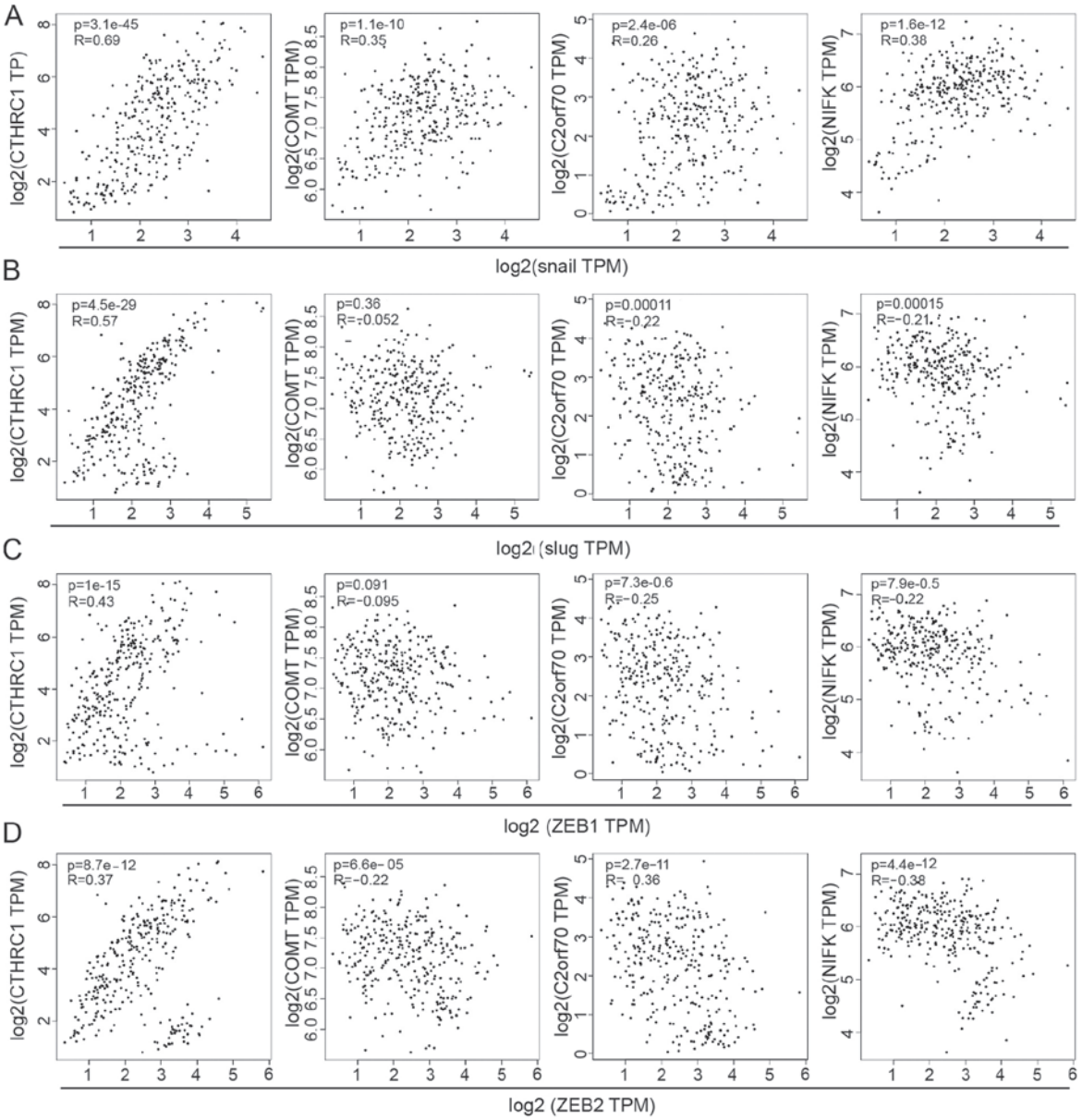

Figure S10. Bioinformatics analysis of CTHRC1. (A) Protein level of CTHRC1 in normal tissue and COAD. (B) mRNA level of CTHRC1 in COAD (red) and normal tissue (grey). (C) mRNA level of CTHRC1 in 31 types of tumors. (D) Patient survival analysis demonstrated that high expression of CTHRC1 predicted a worse OS and DFS rate in COAD. *P<0.05. CTHRC1, collagen triple helix repeat containing 1; COAD, colon adenocarcinoma; OS, overall survival; DFS, disease-free survival.

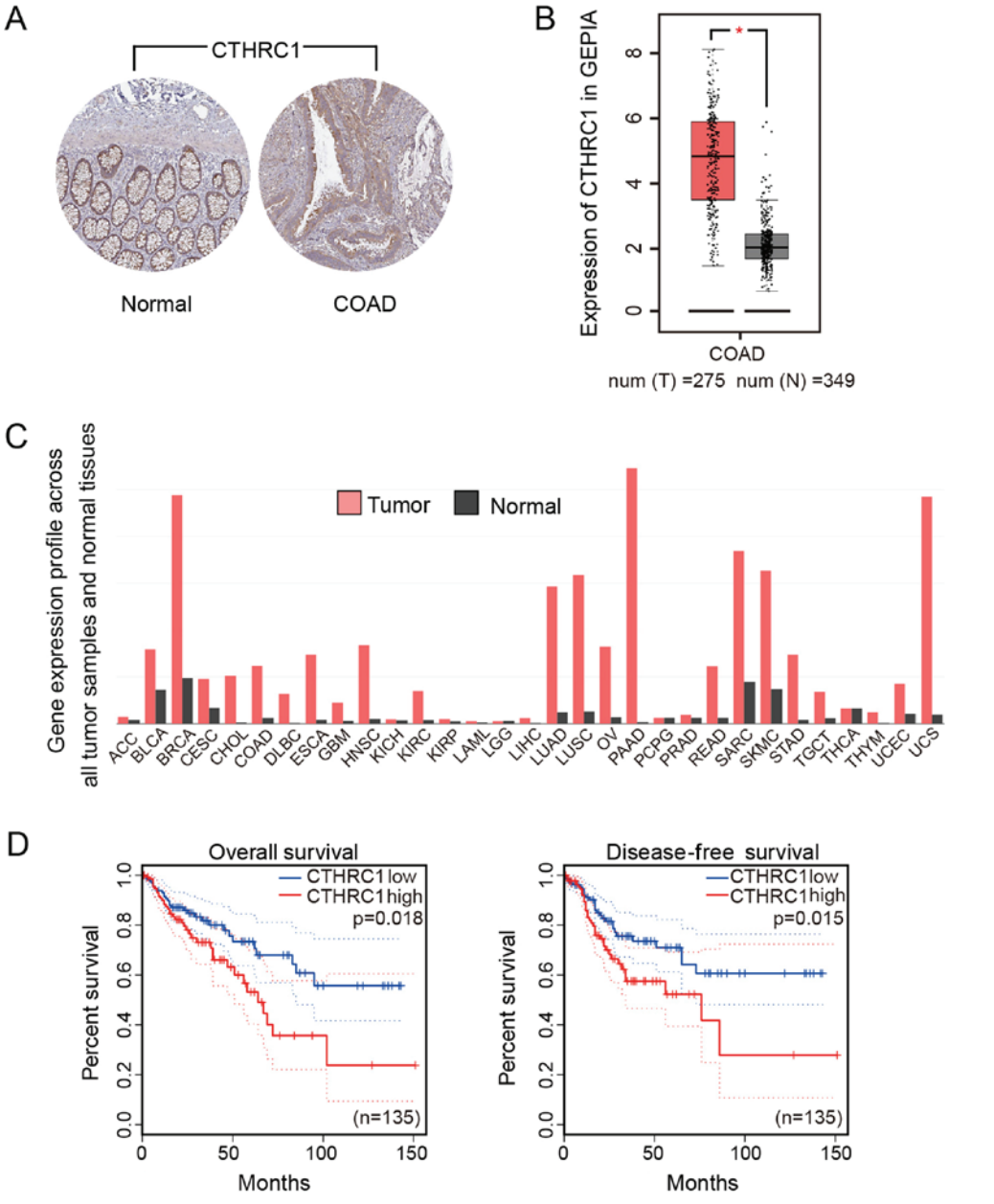

Figure S11. siRNA-mediated knockdown of CTHRC1 in CRC cells detected by western blotting. Data are presented as mean ± standard deviation (n=3). **P<0.01 vs. control group (0 μM CVB-D). CTHRC1, collagen triple helix repeat containing 1; CVB-D, cyclovirobuxine D; siRNA, small interfering RNA,

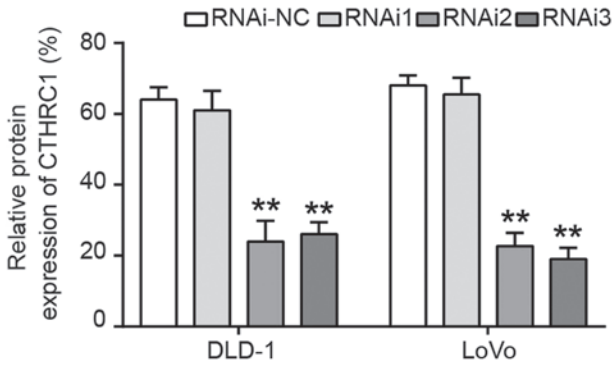

Figure S12. Knockdown of collagen triple helix repeat containing 1 mediated by small interfering RNA in colorectal cancer cells results in the inhibition of p-AKT, p-ERK and Snail. Data are presented as mean ± standard deviation (n=3). **P<0.01 vs. control group (0 μM CVB-D). p-, phosphorylated; NC, negative control; RNAi, interfering RNA; CVB-D, cyclovirobuxine D.

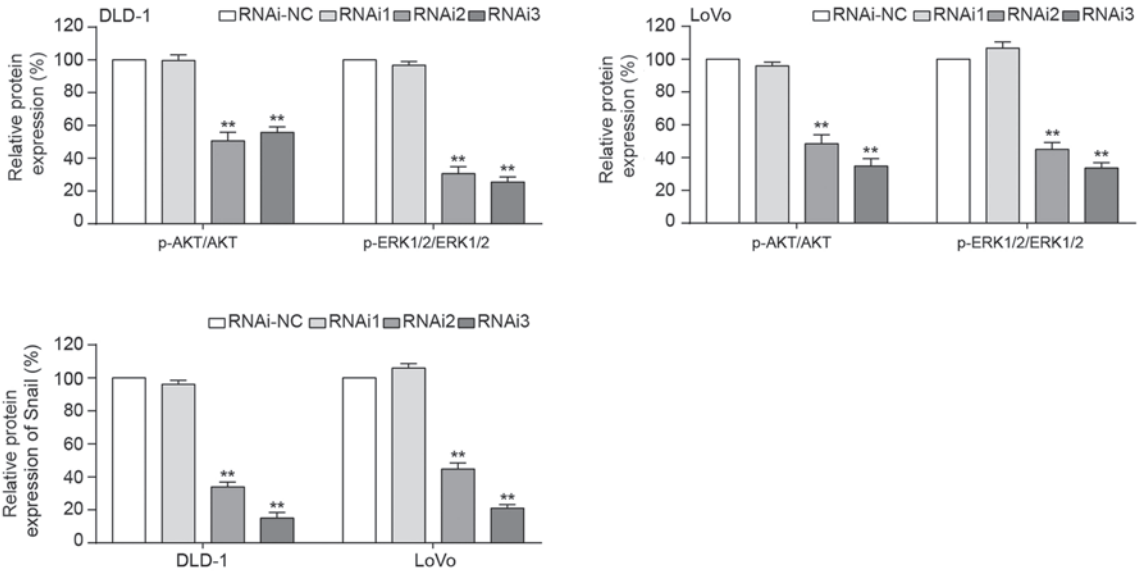

Figure S13. Pathological changes of angiogenesis. Pathological changes of tumor vessels were observed by hematoxylin and eosin staining, which demonstrated that angiogenesis was inhibited by CVB-D (15 mg/kg, once a day for 4 weeks). Magnification, x200. Scale bar, 100 μm. CVB-D, cyclovirobuxine D.

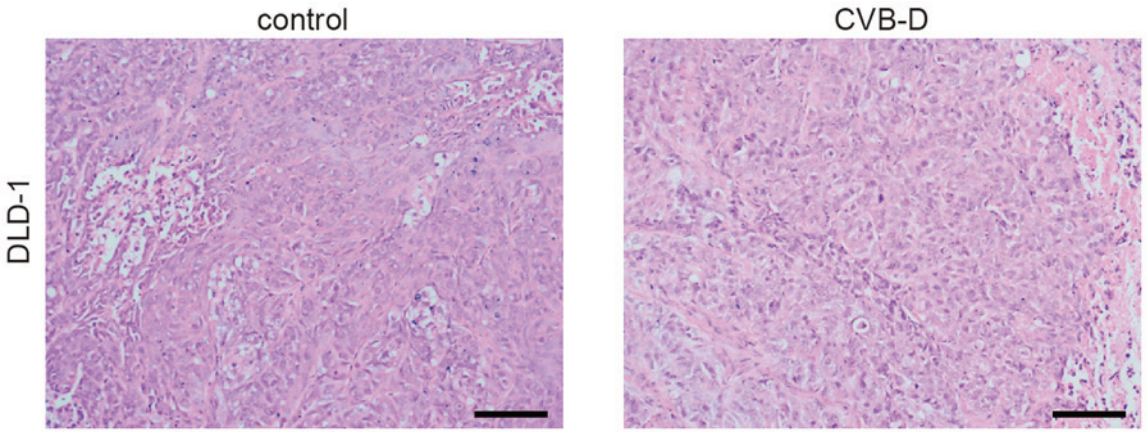

Figure S14. No obvious visceral necrosis was observed in either the experimental or the control group. Hematoxylin and eosin staining was used to observe the pathological changes of the organs of the transplanted mice, and no obvious necrosis was identified. Magnification, x200. Scale bar, 100 μm. CVB-D, cyclovirobuxine D.

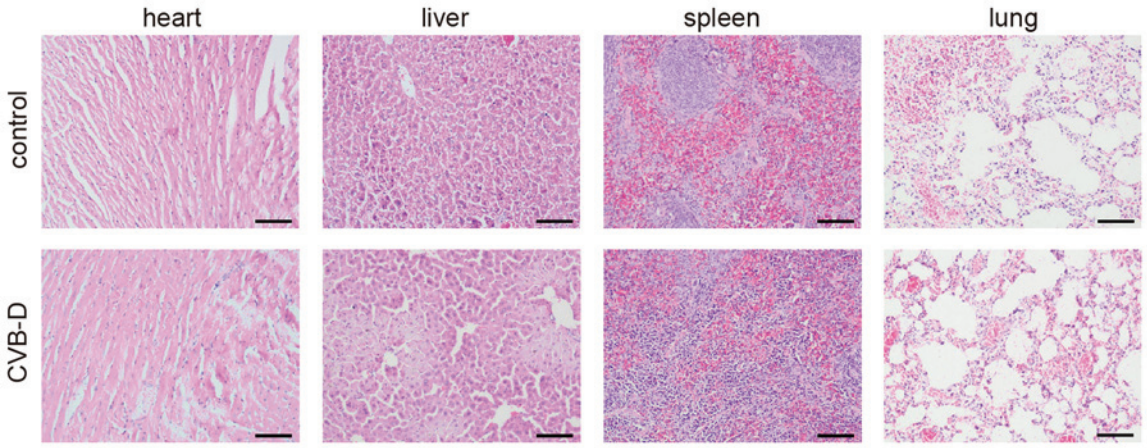

Table SI. Sequences of a control non-targeting siRNA and three collagen triple helix repeat containing 1-targeting siRNAs.

Type of siRNA	Sequence
RNAi-negative control	5'-UUCUCCGAACGUGUCACGUTTACGUGACACGUUCGGAGAATT-3'
RNAi1	5'-GUAUAAUGGAAUGUGCUUATTUAAGCACAUUCCAUUAUACTT-3'
RNAi2	5'-AGGACUUUGUGAAGGAAUUTTAAUUCCUUCACAAAGUCCUTT-3'
RNAi3	5'-UGGCAUAGAUCUUGGGAAATTUUUCCCAAGAUCUAUGCCATT-3'

siRNA, small interfering RNA.